

# Functional Link between BLM Defective in Bloom's Syndrome and the Ataxia-telangiectasia-mutated Protein, ATM\*

Received for publication, April 19, 2002, and in revised form, May 24, 2002  
Published, JBC Papers in Press, May 28, 2002, DOI 10.1074/jbc.M203801200

Heather Beamish<sup>‡§</sup>, Padmini Kedar<sup>¶</sup>, Hideo Kaneko<sup>||</sup>, Philip Chen<sup>‡</sup>, Toshiyuki Fukao<sup>¶||</sup>,  
Cheng Peng<sup>‡</sup>, Sergei Beresten<sup>\*\*</sup>, Nuri Gueven<sup>‡</sup>, David Purdie<sup>‡</sup>, Susan Lees-Miller<sup>‡‡</sup>,  
Nathan Ellis<sup>\*\*</sup>, Naomi Kondo<sup>||</sup>, and Martin F. Lavin<sup>‡§§||</sup>

From the <sup>‡</sup>Queensland Cancer Fund Research Laboratories, The Queensland Institute of Medical Research, P. O. Royal Brisbane Hospital, Herston, Brisbane, Qld 4029, Australia, the <sup>¶</sup>NIEHS, National Institutes of Health, Research Triangle Park, North Carolina, the <sup>||</sup>Department of Pediatrics, Gifu University School of Medicine, 40 Tsukasa-machi, Gifu 500-8076, Japan, the <sup>\*\*</sup>Department of Human Genetics, Memorial Sloan Kettering Cancer Center, New York, New York 10021, the <sup>‡‡</sup>Department of Biological Sciences, University of Calgary, University Drive, Calgary, Canada, and the Departments of <sup>§§</sup>Surgery and <sup>§</sup>Pathology, University of Queensland, Brisbane, Qld 4029, Australia

**Chromosome aberrations, genomic instability, and cancer predisposition are hallmarks of a number of syndromes in which the defective genes recognize and/or repair DNA damage or are involved in some aspect of DNA processing. We report here direct interaction between BLM, mutated in Bloom's Syndrome (BS), and ATM, mutated in ataxia-telangiectasia, and we have mapped the sites of interaction. Full-length BLM cDNA corrected sister chromatid exchange (SCE) and radiosensitivity in BS cells. Mitotic phosphorylation of BLM was partially dependent on ATM, and phosphorylation sites on BLM were identified. A phosphospecific antibody against one of these sites (Thr-99) revealed radiation-induced phosphorylation, which was defective in ataxia-telangiectasia cells. Stable cell lines expressing phosphorylation site mutants failed to correct radiosensitivity in BS cells but corrected SCE. These mutants also sensitized normal control cells to radiation and increased radiation-induced chromosome aberrations but did not cause SCE numbers to increase. These data suggest that ATM and BLM function together in recognizing abnormal DNA structures by direct interaction and that these phosphorylation sites in BLM are important for radiosensitivity status but not for SCE frequency.**

Bloom's syndrome (BS)<sup>1</sup> is characterized by immunodeficiency, infertility, telangiectatic erythema, growth retardation, and chromosome aberrations, including gaps and rearrangements and a predisposition to diabetes, leukemias, and lymphomas (1, 2). Some of these characteristics including chromosomal instability, immunodeficiency, and cancer predisposition are shared with the genome instability syndromes ataxia-tel-

angiectasia (A-T), Nijmegen breakage syndrome (NBS), and Fanconi anemia. Disturbances in DNA metabolism are evident in BS including slow replication fork progression and abnormal distribution of DNA replication intermediates (3, 4). BS cells exhibit hypersensitivity to UV, hydroxyurea, and alkylating agents (5) and a variable sensitivity to ionizing radiation (6). The gene mutated in BS, *BLM*, encodes a 1417-amino acid protein with homology to the RECQ family of helicases including RECQL, Werner Syndrome protein, RECQ4 (mutated in Rothmund-Thomson syndrome), RECQ5, and the yeast proteins Sgs1p and Rqh1p (2, 7–9). Overexpression of BLM and purification from *Saccharomyces cerevisiae* showed that it had ATP-dependent 3'-5'-DNA helicase activity (10, 11). BLM is a nuclear protein present in nuclear bodies containing the promyelocytic leukemia protein (12). It is also localized to diffuse patches in the nucleolus and a subset of telomeres (11, 13). Its localization to the nucleolus coincides with a peak of accumulation in the S phase of the cell cycle (14). During mitosis, BLM is post-translationally modified by phosphorylation followed by a sharp decline in G<sub>1</sub> phase. Immunodepletion of BLM from *Xenopus laevis* extracts leads to inhibition of DNA replication (15), and there is evidence that BLM acts to suppress double strand breaks during replication (16). Although the exact role of BLM remains undefined, it seems likely that it suppresses inappropriate recombination.

The presence of BLM in a multiprotein complex BASC (BRCA1-associated genome surveillance complex) with BRCA1, ATM, several damage repair proteins, and the Mre11/Rad50/Nbs1 complex suggests that it is functionally linked to these proteins (17). Overlapping roles have already been described for members of this complex. *ATM* is mutated in the human genetic disorder A-T (18), *Nbs1* is mutated in Nijmegen breakage syndrome (19–21), and *Mre11* is mutated in A-T-like syndrome (22). Mutations in all three of these genes give rise to a cellular radiosensitive phenotype, and there is evidence that *ATM* and the *Mre11/Rad50/Nbs1* complex function together in recognizing damage in DNA (23–25). *ATM* is a member of the phosphatidylinositol-3 kinase family of proteins that respond to DNA damage by phosphorylating key substrates involved in DNA repair and/or cell cycle control (26, 27). Activation of *ATM* by double strand breaks in DNA leads to rapid phosphorylation of p53 and Chk2 and subsequent activation of cell cycle checkpoints (28–32). p53 is phosphorylated on serine 15 directly by *ATM* and on serine 20 by Chk2 in an *ATM*-dependent manner as part of the stabilization/activation of this molecule to ulti-

\* This work was supported by grants from the Australian National Health and Medical Research Council, the Queensland Cancer Fund, and the A-T Children's Project. This work was also supported in part by the Australian-Japan Cooperative Research Program and the Uehara Research Foundation. The costs of publication of this article were defrayed in part by the payment of page charges. This article must therefore be hereby marked "advertisement" in accordance with 18 U.S.C. Section 1734 solely to indicate this fact.

<sup>¶¶</sup> To whom correspondence should be addressed. Tel.: 61-7-3362-0341; Fax: 61-7-3362-0106; E-mail: martinL@qimr.edu.au.

<sup>1</sup> The abbreviations used are: BS, Bloom's Syndrome; A-T, ataxia-telangiectasia; ATM, ataxia-telangiectasia-mutated; NBS, Nijmegen breakage syndrome; SCE, sister chromatid exchange; GST, glutathione S-transferase; DTT, dithiothreitol; BASC, BRCA1-associated genome surveillance complex.

mately bring about arrest of cells in G<sub>1</sub> phase (31, 33). It has also been demonstrated that ATM-dependent activation of Chk2 requires Nbs1 (34). ATM phosphorylation of Nbs1 on serine 343 is required for radiation-induced activation of the S phase checkpoint, and mutations in either of these proteins give rise to radioresistant DNA synthesis (23, 35). On the other hand, BRCA1 function is required for both the S phase and G<sub>2</sub>/M checkpoints with ATM phosphorylation of BRCA1 on serine 1423 implicated in the G<sub>2</sub>/M checkpoint (36). Although it is evident that ATM and BLM recognize abnormal structures in DNA and suppress aberrant recombination, it is unclear as to whether they overlap at the mechanistic level. In this report we show that BLM interacts directly with ATM, BS cells exhibit radiosensitivity, and that the mitotic hyperphosphorylation of BLM is partially ATM-dependent, and we identify ATM-dependent phosphorylation sites on BLM that are phosphorylated post-irradiation in a dose-dependent manner. Mutation of either of these two sites alters survival and chromosome aberrations in response to radiation in transfected control cells and fails to correct radiosensitivity in BS cells.

#### EXPERIMENTAL PROCEDURES

**Cell Survival**—Cells were plated at 10<sup>6</sup>/ml in RPMI 1640 for 24 h prior to incubation with CdCl<sub>2</sub> (5 μM) for 48 h prior to exposure to ionizing radiation (0–4 grays). Cell viability was determined by adding 0.1 ml of 0.4% trypan blue to a 0.5-ml cell suspension. The number of viable cells was determined at 72 h post-irradiation. The BS cell lines HG1525, derived from 81(MaGrou), and HG2703, derived from NR2(CrSpe), are from the Bloom's Syndrome Registry.

**Induced Chromosome Aberrations**—Cells were irradiated with 1 gray of γ-rays and incubated with Colcemid (0.1 μg/ml) for 2 h prior to harvesting. The cells were treated for 15 min in 0.075 M KCl, fixed in methanol/glacial acetic acid, 3:1 (v/v), and spread on glass slides. The cells were then stained with Giemsa, and 50 metaphases were analyzed for each sample.

**SCE Analysis**—Differential staining of sister chromatids in metaphases was performed as described previously (2).

**Fluorescence-activated Cell Sorter Analysis**—Cell cycle distribution after nocodazole was determined as described previously (35) using flow cytometry with propidium iodide staining for DNA.

**Expression and Purification of the GST-BLM Fragments**—Four overlapping reverse transcription-PCR fragments with *Xho*I sites included in the primers were generated to cover the entire BLM open reading frame: BLM1 (1–1154), BLM2 (1070–2177), BLM3 (1978–3297), and BLM4 (3246–4328). A detailed description of the constructs is available from the authors upon request. These were cloned into the *Xho*I site of the GST expression vector pGEX-4T-1. The GST clones were transfected into BL21 cells, and expression was induced by the addition of 0.3 mM isopropyl-1-thio-β-D-galactopyranoside for 4 h. GST fusion proteins were expressed, purified, and eluted with reduced glutathione (6 mg/ml) as described previously (30). For ATM kinase analysis, GST-BLM 1, 2, 3, and 4 were thrombin-digested (1 unit, Amersham Biosciences) for 2 h at room temperature in phosphate-buffered saline and purified from 10% SDS-PAGE. The gel was reversibly stained with zinc, and the appropriate band was excised, destained in 0.1 M EDTA/phosphate-buffered saline, and eluted into elution buffer (0.05 M Hepes, pH 8, 0.1% SDS, 0.5 mM EDTA, 5 mM DTT). The resulting protein was acetone-precipitated and resuspended in H<sub>2</sub>O.

**Antibody Production**—The BLM-specific antibody, BLM1BA, was raised against GST-BLM fusion proteins 1 and 4 purified from SDS-PAGE and injected into sheep with Freund's complete adjuvant. The animal was given four booster shots at 4-week intervals, and the sheep were bled 7 and 14 days after the third and fourth boost. The crude antisera was tested against the preimmune sera for BLM specificity. Antibody was purified using GST-BLM affinity chromatography. Phosphospecific antibody against Thr-99 BLM was generated by inoculation of a phosphorylated peptide (KNAPAGQE Phospho-TQRGGSKSLC) into rabbits (IMVS Adelaide). Antisera was purified by first passing through a column containing non-phosphorylated peptide coupled to a thiopropyl-Sepharose 6B gel and subsequently purified on a phosphopeptide-Sepharose column (Mimotopes, Melbourne, Australia).

**Western Blotting, Immunoprecipitation, and Antibodies**—Whole cell extracts were made from control (C3ABR), A-T (AT1ABR, AT3ABR,

L3), and BS (HG1525, HG2703, GM 3403F) lymphoblastoid cell lines as described previously. Briefly, cells were lysed in TGN buffer (50 mM Tris-HCl (pH 7.4), 50 mM β-glycerophosphate, 150 mM NaCl, 10% glycerol, 1% Tween, 1 mM NaF, 1 mM sodium orthovanadate, 1 mM phenylmethylsulfonyl fluoride, 2 μg/ml pepstatin, 5 μg/ml leupeptin, 10 μg/ml aprotinin, 1 mM DTT) on ice for 30 min, cellular debris was removed by centrifugation for 15 min at 4 °C, and protein concentration was determined by the DC protein kit (Bio-Rad) as per the manufacturer's instructions. For immunoblotting, 100 μg was used. For co-immunoprecipitation assays, 1 mg of each extract was precleared with 50 μl of protein A/G-Sepharose 50% slurry and then immunoprecipitated with 10 μg of either ATM5BA or BLM1BA at 4 °C for 2–16 h. The immune complex was purified by the addition of 50 μl of protein A/G-Sepharose and mixed for a further 2 h. The immune complexes were washed five times with TGN, three times with TGN/0.2% Triton, and two times with TGN/0.5% Triton, eluted into Laemmli buffer, and separated on a 4.2% SDS-polyacrylamide gel, transferred to nitrocellulose, and probed with either ATM5BA or BLM1BA. To synchronize the cells in the M phase of the cell cycle, 0.4 μM nocodazole was incubated with exponentially growing cells for 16 h. Cells were released into fresh RPMI 1640/10% fetal calf serum medium, and the cell cycle was followed using fluorescence-activated cell sorter analysis. At 1 h post-release, when the cells were determined to be in G<sub>2</sub>/M phase of the cell cycle, whole cell extracts were prepared as described above, 100 μg of protein was loaded onto a 4.2% SDS-polyacrylamide gel, and the sample was Western blotted for BLM. Antibodies used in this study were as follows: ATM-2C1 (GeneTex), Phospho-p53 (Ser-15) (Cell Signaling Technology), BRCA1 (Calbiochem), DNA-dependent protein kinase catalytic subunit (DNA-PKcs) (Oncogene), nibrin (Novus), and actin (Sigma).

**Co-purification**—ATM was cloned into pMEP4 and expressed in AT3ABR as described previously (37). Cells were exposed to 5 μM CdCl<sub>2</sub> for 16 h, and whole cell lysates were prepared as described. The recombinant ATM protein was first purified on a HiTrap chelating column (Amersham Biosciences), washed twice with TGN, and eluted with increasing imidazole concentration (25, 50, 75, 100 mM) in TGN. Elutions were prepared by boiling with Laemmli buffer and then separated on a 4.2% SDS-polyacrylamide gel, transferred to nitrocellulose, and probed with antibodies ATM5BA or BLM1BA.

**GST Binding**—12 overlapping GST-ATM constructs as described previously (30) were used, as were the four BLM GST constructs. For *in vitro* transcription/translation, full-length ATM was cloned into pBS, as was the full-length BLM. Both BLM and ATM were translated *in vitro* using the TnT-coupled transcription/translation kit (Promega). GST-ATM fusion proteins (5 μg) were incubated with *in vitro* transcribed and translated [<sup>35</sup>S]methionine-labeled BLM protein in binding buffer (20 mM Tris, pH 7.4, 100 mM NaCl, 1 mM EDTA, 1 mM DTT, 0.1% Nonidet P-40) either with or without EtBr (50 μg/ml) for 1 h at 4 °C, and then washed in wash buffer (20 mM Tris, pH 7.4, 100 mM NaCl, 1 mM EDTA, 1 mM DTT, 0.25% Nonidet P-40, 10% glycerol). GST-BLM fusion proteins (5 μg) were incubated with *in vitro* transcribed and translated [<sup>35</sup>S]-labeled ATM protein in binding buffer with EtBr for 1 h at 4 °C and then washed in wash buffer as described. The bound proteins were analyzed by SDS-PAGE followed by fluorography.

**In Vitro Mutagenesis**—Two site-directed mutations were generated in the BLM GST-1 fragment. Both Thr-99 and Thr-122 were mutated by the QuikChange site-directed mutagenesis kit (Stratagene) as per the manufacturer's instructions.

Primer 1 (5'-AGCAGGACAGAAGCACAGAGAGGTGGATC-3') and Primer 2 (5'-TCGTCCTGTCTTCGTGTCTCTCCACCTAG-3') were used to mutate Thr-99. Accordingly, Primer 3 (5'-GAAGTTGTATGCATGCCAAACACACCA-3') and Primer 4 (5'-CTTCAACATACGTGACGGGTTTGTGTGTGT-3') were used to mutate Thr-122.

**ATM Kinase Assay**—ATM kinase assays were performed as described previously (29). Briefly, 1 mg of whole cell extract was precleared for 30 min with rotation at 4 °C with 50 μl of a 50% v/v slurry of protein A/G-Sepharose. 2 μl of ATM5BA crude serum was added, and the complex was rotated for a further 2 h, and then the complex was removed by addition of 50 μl for the protein A/G-Sepharose mix and rocked for another hour. The complex was washed three times with TGN, once with 0.5 M LiCl, 100 mM Tris-HCl (pH 7.4), and twice with kinase buffer (10 mM Hepes (pH 7.5), 50 mM β-glycerophosphate, 50 mM NaCl, 10 mM MgCl<sub>2</sub>, 10 mM MnCl<sub>2</sub>, 5 μM ATP, 1 mM DTT). Half of this reaction was removed and run on a 4.2% polyacrylamide gel and Western blotted for the amount of ATM present in the immunoprecipitation. The remaining pellet was resuspended in 20 μl of kinase buffer with the addition of 1 μg of substrate and 10 μCi of [γ-<sup>32</sup>P]ATP and incubated at 30 °C for 30 min followed by the addition of 5 μl of 5× Laemmli buffer

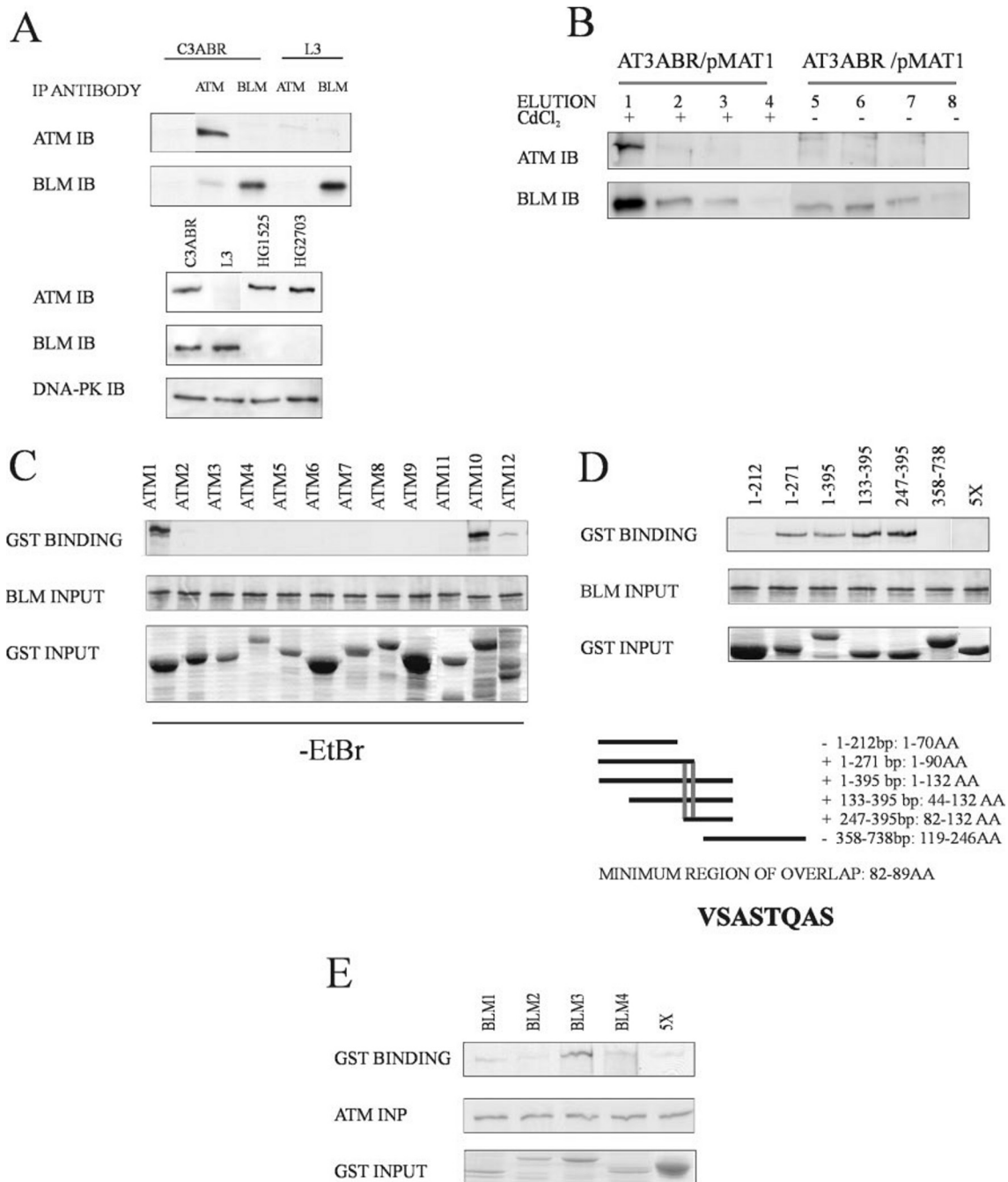


FIG. 1. **BLM interacts directly with ATM.** *A*, whole cell extracts (5 mg) from control (C3ABR) and A-T (L3) cells were immunoprecipitated (IP) with antibodies against ATM (ATM5BA), BLM, or nonspecific antibody followed by immunoblotting (IB) for ATM and BLM (upper panel). Immunoblotting was also carried out with extracts prepared from the C3ABR, L3, and 2 BS cell lines (HG1525, HG2703) for ATM and BLM. Loading was determined using an antibody to DNA-PK. *B*, use of nickel chelate chromatography to demonstrate binding of ATM and BLM. AT3ABR cells stably transfected with full-length hexahistidine-tagged ATM cDNA (pMAT1) were induced to express ATM with CdCl<sub>2</sub> prior to application to a nickel chelate column. Bound protein was eluted with imidazole. Lanes 1–4 and lanes 5–8 represent 25, 50, 75, and 100 mM imidazole elutions. Eluted samples were separated on a 4.2% SDS-PAGE and immunoblotted with ATM5BA and BLM1BA antibodies. *C*, BLM binding to GST-ATM fusion proteins. *In vitro* transcription/translated [<sup>35</sup>S]methionine-labeled BLM was incubated with 5  $\mu$ g of ATM GST fusion proteins covering the length of ATM (30). Binding was determined on 4.2% SDS-PAGE followed by fluorography. BLM input lanes represent 10% of the label used in binding. Amounts shown for ATM GST input are those used in the binding. *D*, fine mapping of BLM binding to GST-ATM1. Numbers represent nucleotides of ATM from the N terminus, and 5X represents pGEX only. AA, amino acids. *E*, ATM binding to GST-BLM fusion proteins. As described for panel C, ATM was labeled with [<sup>35</sup>S]methionine prior to binding to BLM GST fragments 1–4 from the N-terminal end.

(5% SDS, Tris-HCl (pH 6.8),  $\beta$ -mercaptoethanol, bromophenol blue), heated to 95 °C for 5 min, and run on a 10% polyacrylamide gel. The resulting gel was stained with bromophenol blue to check the loading of the substrate followed by autoradiography.

#### RESULTS

**BLM Interacts Directly with ATM**—The phenotype observed in BS suggests that BLM plays a role in recognizing abnormal

structures in DNA and suppressing recombinational events that lead to genomic instability. To understand more fully the role of BLM in maintaining genomic stability, we initially employed the yeast two-hybrid system to identify proteins that interact with and influence the function of BLM. Full-length BLM cDNA was divided into two overlapping fragments and was PCR-cloned into the yeast-pA22 vector containing the Gal4



DNA-binding domain, pGBT9-R1 (nucleotides 1998–4328) and pGBT9-A8 (nucleotides 72–2084). pGBT9-A8 was found to self-activate and was thus discarded. Following sequential transformation of the yeast strain Y190 with pGBT9-R1 and a cDNA library (human leukemia matchmaker DNA library) fused with the Gal4 activation domain vector pG6AD10,  $3 \times 10^6$  independent clones were screened on leu<sup>-</sup> trp<sup>-</sup> his<sup>-</sup> plates in the presence of 3-amino-1,2,4-triazole, and the resultant colonies were further screened using the  $\beta$ -galactosidase filter assay leading to the identification of five positive clones. Sequence analysis of two strongly positive clones (3F3 and 3C5) identified a 5.5-kb fragment from the C terminus of ATM (ataxia-telangiectasia-mutated) cDNA (3F3) and BLM cDNA (3C5). Self-interaction is in keeping with results showing that BLM forms hexameric ring structures (38).

To confirm the interaction of BLM with ATM, we employed co-immunoprecipitation and co-purification on nickel chelate chromatography. When extracts from control cells (C3ABR) were immunoprecipitated with ATM5BA antibody and immunoblotted with anti-BLM antibody, BLM was shown to associate with ATM (Fig. 1A, upper panel). As expected, similar immunoprecipitates from the A-T cell line L3, which does not express ATM (39), showed no evidence of co-immunoprecipitation nor did a control antibody immunoprecipitate BLM (Fig. 1A, upper panel). Immunoblots reveal the relative amounts of ATM and BLM proteins in the different cell lines (Fig. 1A, lower panel). Reciprocal experiments were carried out using anti-BLM antibody, but this failed to show evidence of association, presumably because the antibody recognition site interfered with the ATM/BLM interaction. Consequently we used an alternative approach to look for association in AT3ABR cells expressing ATM containing a hexahistidine sequence (pMAT1). These cells were stably transfected with ATM cDNA and induced with CdCl<sub>2</sub> to express ATM as described previously (37). Extracts were applied to a nickel chelate resin, and ATM was eluted with imidazole, run on an SDS-polyacrylamide gel, and immunoblotted with anti-ATM and BLM antibodies. Again as observed with co-immunoprecipitation, there was evidence for the association of ATM and BLM (Fig. 1B, lanes 1–4) with BLM preferentially eluted in the same elution fraction as ATM after CdCl<sub>2</sub> induction of the ATM levels. There was no evidence of ATM/BLM interaction in the absence of induction (Fig. 1B, lanes 5–8). The background levels of BLM in the uninduced samples (lanes 5–8) are due to some nonspecific binding of BLM to the nickel chelate column.

To map the regions of interaction, we used a series of 12 GST-ATM fusion proteins representing the complete ATM protein (30). Binding was determined with <sup>35</sup>S-labeled *in vitro* transcribed and translated full-length BLM in the presence and absence of ethidium bromide to minimize the likelihood of interaction through DNA. BLM bound to GST-ATM-1 (amino acid residues 1–257), GST-ATM-10 (residues 2427–2641), and GST-ATM-12 (residues 2682–3012) in reactions without ethidium bromide (Fig. 1C). However, when this compound was included, GST-ATM-1 and GST-ATM-12 were found to bind equally well to BLM, but there was reduced interaction with GST-ATM-10 (results not shown). Binding of BLM to GST-ATM-10–12, which contains the kinase domain of ATM, is consistent with this protein being a substrate for ATM kinase. The binding of BLM to GST-ATM-1 was strongest (~50% of the input). To map in more detail the region of interaction on ATM-1, we prepared a number of small overlapping GST fusion proteins within this area. Binding studies with <sup>35</sup>S-labeled BLM revealed that the smallest region of overlap was a sequence of ~24 nucleotides, which corresponds to amino acids

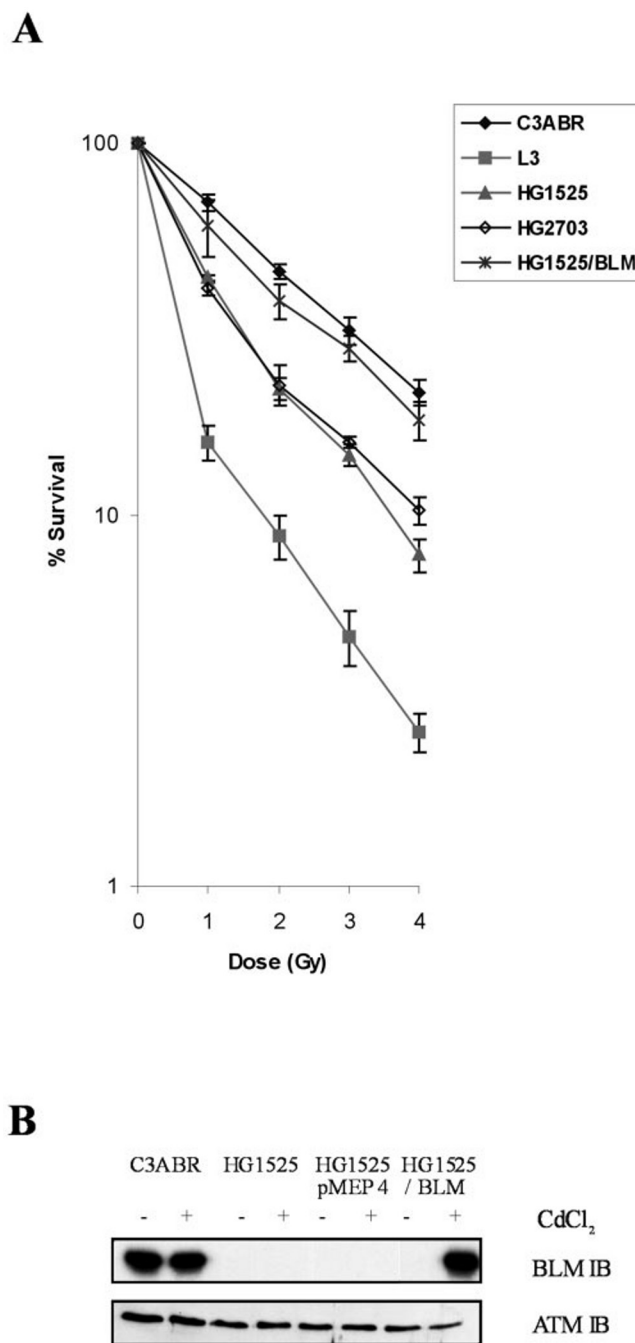


**FIG. 2. Correction of radiosensitivity in BS cells.** A, cell survival at day 3 after irradiation as determined by trypan blue exclusion. C3ABR, control; L3, A-T; HG1525 and HG2703, BS. Vector only transfected BS cells, HG1525/pMEP4, and BS cells transfected with full-length BLM cDNA, HG1525/BLM. Gy, grays. B, stably transfected BS cells with either vector only (HG1525/pMEP4) or full-length BLM (HG1525/BLM) were incubated with CdCl<sub>2</sub> (+), and extracts were prepared 48 h later. Extracts were immunoblotted (IB) with either BLM antibody or ATM5BA.

82–89 (Fig. 1D). It is of some interest that the strongest binding site on ATM for p53 and BRCA1 also maps to this region (30, 40). Mapping the region of interaction in BLM was carried out using four overlapping GST fusions (GST 1–4, numbered from the N-terminal end). Binding of GST-BLM-3 amino acid residues 636–1074 to <sup>35</sup>S-labeled full-length ATM was observed (Fig. 1E). Addition of ethidium bromide did not alter this pattern of binding (results not shown).

**Correction of SCE and Radiosensitivity in BS Cells**—A major characteristic of A-T cells is extreme sensitivity to ionizing

TABLE I  
SCE and correction in transfected cells

Control (C3ABR) and BS (HG1525) cells were stably transfected as indicated, and SCE/metaphase was determined after induction with CdCl<sub>2</sub>. *P* values for HG1525 transfected cells represent a comparison with SCEs in the parental untransfected line (HG1525). Values are not provided for C3ABR transfected cells, but they are all significantly lower than BS cells. pMEP4 is the empty vector, BLM is wild type BLM in the vector, and Thr-99(A) and Thr-122(A) represent mutant forms of BLM. *N* is the number of metaphases scored. L3 is an A-T cell line. CI, confidence interval.

Cell line	<i>N</i>	SCE metaphase	Standard error	Lower 95% CI for mean	Upper 95% CI for mean	<i>P</i> value (Wilcoxon test)
C3ABR	10	6.80	0.36	5.99	7.61	
C3ABR+pMEP4	10	2.90	0.28	2.27	3.53	
C3ABR+BLM	8	3.88	0.48	2.74	5.01	
C3ABR+Thr-99(A)	12	2.69	0.26	2.12	3.26	
C3ABR+Thr-122(A)	20	3.40	0.27	2.84	3.96	
C3ABR+Thr-99/122	12	7.58	1.01	5.36	9.81	
HG1525	10	75.70	6.27	61.52	89.88	
HG1525+pMEP4	12	63.08	4.71	52.72	73.44	
HG1525+BLM	19	12.32	1.42	9.33	15.30	<0.0001
HG1525+Thr-99(A)	20	17.65	3.04	11.30	24.00	<0.0001
HG1525+Thr-122(A)	17	26.82	3.60	19.19	34.45	<0.0001
L3	8	9.5				

TABLE II  
Correction of radiation-ICA

Control (C3ABR) and BS (HG1525) cells were stably transfected as indicated, and ICA/metaphase, was determined. sb, chromatid breaks, cb, chromosome breaks; Int, interchanges, *N*, the number of metaphases scored. Transfected cells are the same as described in Table I legend. The ICA values for control and A-T cells over a series of seven independent experiments are  $0.92 \pm 0.11$  (C3ABR) and  $3.03 \pm 0.09$  (A-T, L3). CI, confidence interval.

Cell line	sb	cb	Int	<i>N</i>	ICA/metaphase	Standard error	Lower 95% CI for mean	Upper 95% CI for mean	<i>P</i> value (Wilcoxon test)
C3ABR	43	2	1	49	0.94				
C3ABR+pMEP4	46	0	0	50	0.92				
C3ABR+BLM	42	0	0	50	0.84				
C3ABR+Thr-99(A) <sup>a</sup>	102	0	1	50	2.10	0.25	1.59	2.61	0.017
C3ABR+Thr122(A) <sup>a</sup>	86	1	0	50	1.74	0.20	1.34	2.14	0.024
C3ABR+Thr99/122(A) <sup>a</sup>	82	0	1	50	1.66	0.25	1.16	2.16	0.026
HG1525	110	2	3	50	2.30	0.28	1.73	2.87	
HG1525+pMEP4 <sup>b</sup>	125	0	1	50	2.52	0.29	1.93	3.11	0.624
HG1525+BLM <sup>b</sup>	67	1	1	51	1.35	0.22	0.92	1.79	0.012
L3	152	0	1	50	3.06				

<sup>a</sup> Compared with C3ABR.

<sup>b</sup> Compared with HG1525.

radiation (41). Since we had shown that BLM and ATM interact, it was possible that this interaction might influence the radiation response and that loss of BLM in BS cells might exacerbate this response. It is clear from the results in Fig. 2A that HG1525 and HG2703 cells are intermediate between control and A-T cells in radiosensitivity. These two cell lines are characteristic of BS cells with elevated SCE in the unirradiated state, HG1525 (75.7 SCE/46 chromosomes) and HG2703 (82.5 SCE/46 chromosomes) as compared with three to seven in controls (Table I). To test the specificity of these observations, we stably transfected BS cells with an Epstein-Barr virus-based vector expressing full-length BLM under the control of an inducible metallothionein promoter (HG1525/BLM). Incubation of transfected cells with CdCl<sub>2</sub> led to an induction of BLM to a level comparable with that expressed in control cells (Fig. 2B). This level of expression enhanced the radioresistance of BS cells to that in controls (Fig. 2A). Radiation-induced chromosome aberrations in BS cells were also reduced after transfection with full-length BLM cDNA from 2.0 to 1.35 induced chromosome aberrations/metaphase (Table II). The induced chromosome aberration value for controls is  $0.92 \pm 0.11$ , whereas that for A-T is  $3.03 \pm 0.09$ .

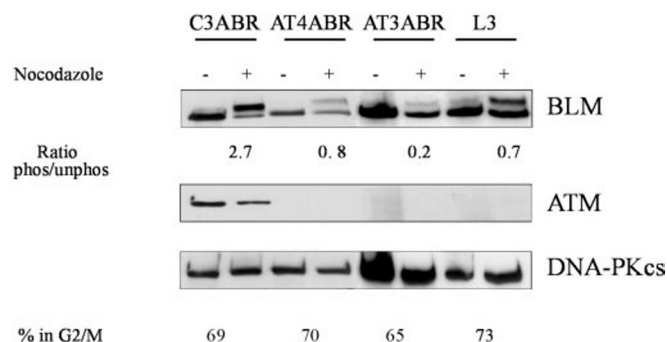
**Mitosis-associated Phosphorylation of BLM Is ATM-dependent, and ATM Phosphorylates BLM at Two Sites**—Since BLM is hyperphosphorylated in mitosis (14), we determined whether this phosphorylation was ATM-dependent and what sites were involved. Cells were blocked in G<sub>2</sub>/M with the microtubule-stabilizing agent, nocodazole, released and harvested 1 h later, and immunoblotting for BLM was carried out. The results in

Fig. 3 demonstrate that the majority of BLM exists in a hyperphosphorylated form (retarded species) for control cells at 1 h after release from nocodazole (69% G<sub>2</sub>/M cells). The ratio of phosphorylated to unphosphorylated BLM was ~3 for the control cell line and 2 for a second control (results not shown). On the other hand, in three A-T cell lines examined, the greatest proportion of BLM was in the hypophosphorylated form at 1 h after release with the ratio of the two forms ranging from 0.2 to 0.8 (65–73% G<sub>2</sub>/M cells). Since we showed that BLM interacts directly with ATM, we determined whether BLM was a substrate for ATM kinase. To address this, we employed the four overlapping GST-BLM fusion proteins (described above) as substrates for immunoprecipitated ATM. The results in Fig. 4A, *upper panel*, demonstrate that only the GST-BLM-1 (N-terminal) fragment is phosphorylated by ATM kinase. When immunoprecipitates from an A-T cell line, L3, were used, no kinase activity was observed (Fig. 4A, *lower panel*). Based on consensus sequences described by Kim *et al.* (42), two potential phosphorylation sites (TQ 99–101; TQ 122–123) were identified in the BLM N-terminal peptide for ATM kinase (Fig. 4B). A chromatographically purified N-terminal fragment of BLM (amino acids 1–200) was also efficiently phosphorylated by ATM (Fig. 4C). Mutation of Thr-99 to glycine resulted in a significant reduction in phosphorylation of the thrombin-cleaved GST fusion protein by ATM, indicating that this was a major site for ATM kinase *in vitro*. Residual phosphorylation suggests that Thr-122 is also phosphorylated to a lesser extent. When cells were exposed to radiation, there was an enhancement of ATM kinase activity over a 2-h incubation period using

the GST-BLM fragment as substrate (Fig. 4D). However, as expected, when a fragment with mutated Thr-99 was employed, radiation did not lead to phosphorylation. Yet when Thr-122 was mutated, reduced phosphorylation was still evident (Fig. 4D). Under these conditions, increased phosphorylation of the p53<sub>1-44</sub> fragment was observed. Comparable levels of ATM protein were demonstrated by immunoblotting the immunoprecipitated material. The specificity of this phosphorylation was confirmed using immunoprecipitated ATM from an A-T mutant (AT1ABR) that failed to phosphorylate BLM above basal levels. It is of interest that the basal level of ATM

kinase is elevated in the BS cell line (HG2703) and decreases initially in response to radiation (Fig. 4D).

**Functional Significance of Phosphorylation Sites**—Since ATM was capable of phosphorylating BLM on Thr-99 most efficiently *in vitro*, we prepared a phosphospecific antibody against this site to determine its functional significance. BLM was immunoprecipitated from extracts of control cells with or without radiation exposures prior to immunoblotting with anti-BLM antibody. The results in Fig. 5 demonstrate a low basal level of phosphorylation on Thr-99 of BLM, which increased with increasing radiation dose. It is evident that this is ATM-dependent since the response is much reduced in A-T cells (Fig. 5). Immunoprecipitation with anti-BLM antibody showed normal levels of BLM in control and A-T cells. There is an indication that BLM protein decreases in amount with high radiation dose in A-T cells, but this does not account for failure to observe BLM phosphorylation. As a further test of functional significance, we employed Thr-99 and Thr-122 mutant forms to establish stable cell lines. Expression of either the Thr-99 or Thr-122 mutants in BS cells failed to correct radiosensitivity, whereas normal full-length BLM cDNA restored survival to normal levels (Fig. 6A). However, as for full-length BLM, both mutants reduced SCE levels to those observed in control cells, providing evidence for a dissociation of SCE and DNA damage-induced aberrations. When introduced into control cells, full-length BLM did not alter the phenotype, but the Thr-99 and Thr-122 mutants sensitized these cells to radiation to an extent intermediate between control and A-T (Fig. 6B) and caused a significant elevation in the number of radiation-induced chromosome aberrations (Table II). The double mutant also led to increased aberrations. However, none of the mutants increased



**FIG. 3. Mitotic phosphorylation of BLM is ATM-dependent.** Cells were synchronized using the microtubule inhibitor nocodazole (0.4  $\mu$ M) for 16 h and then released into fresh medium for 1 h prior to harvesting. Extracts were immunoblotted for BLM/ATM and DNA-PKcs as a loading control on a 4.2% SDS-PAGE gel. The ratio of phosphorylated (upper band) to unphosphorylated (lower band) was determined using a PhosphorImager. The percentage of cells in the G<sub>2</sub>/M phase of the cell cycle is shown.

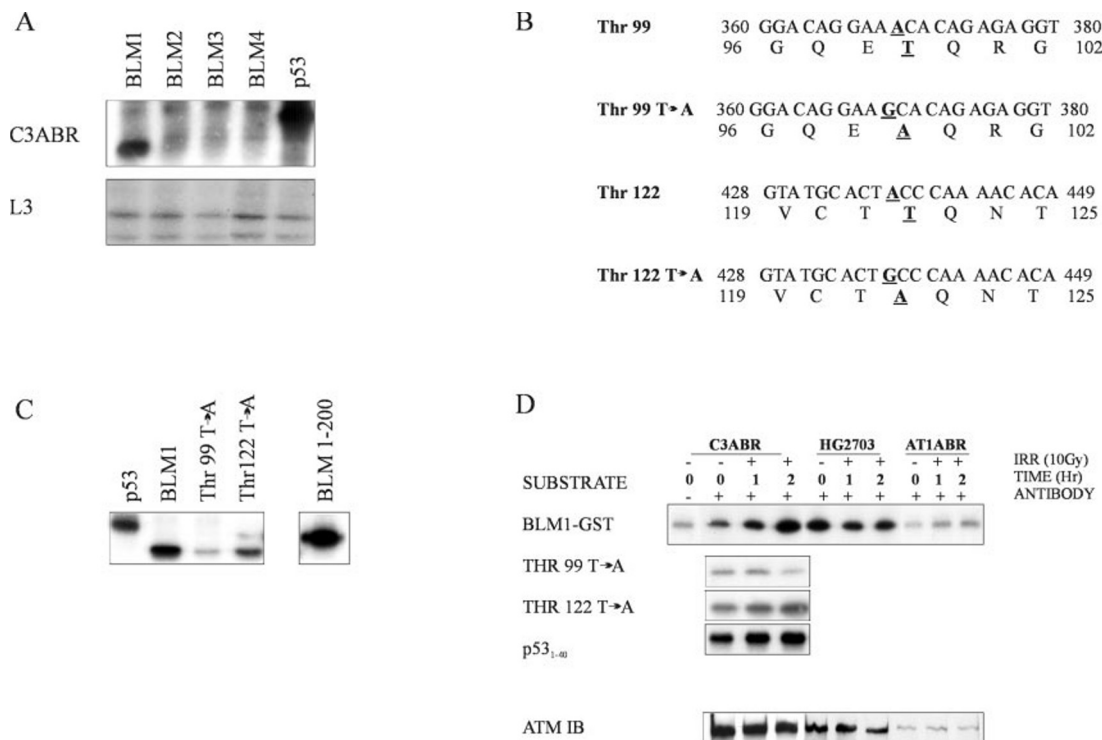


**FIG. 4. BLM is a substrate for ATM kinase.** A, phosphorylation of GST-BLM fusion proteins. ATM was immunoprecipitated from control extracts, and ATM kinase activity was determined using the GST-BLM fusion proteins 1–4 and p53<sub>1-44</sub> (upper panel). Immunoprecipitates were also prepared from A-T (L3) cell extracts using the same substrates to determine ATM kinase activity (lower panel, overexpressed). B, mutation of the two potential ATM kinase sites in GST-BLM1 site 1. 98-ETQR-101 was mutated to EAQR by mutating nucleotide 369 (an A to a G). In site 2, 121-TTQN-124 was mutated to TAQN by mutating nucleotide 437 (an A to a G). C, ATM kinase activity with BLM and mutated fragments. BLM1, GST-BLM1 (N-terminal fragment); Thr-99 T→A, Thr-99 Thr → Ala within BLM1; Thr-122 T→A, Thr-122 Thr → Ala within BLM1 and a purified N-terminal peptide, amino acids 1–200 (BLM 1–200). D, radiation-induced phosphorylation of BLM1 fragments. Extracts were prepared from C3ABR, HG2703, and AT1ABR cells at 0, 1, and 2 h post-irradiation (10 grays), and ATM kinase activity was determined. Activity was also determined using the two mutated fragments (Thr-99 Thr → Ala and Thr-122 Thr → Ala) and p53<sub>1-40</sub>. Loading was determined by immunoblotting of immunoprecipitated ATM.



SCE levels (Table I), again supporting a separation of SCE and chromosome aberration effects.

#### DISCUSSION

We have provided evidence for a functional relationship between the products of two genes that, when mutated, give rise to the human disorders (A-T and BS) characterized by genome instability, immunodeficiency, and cancer predisposition (2, 41). Although these are distinct diseases, the BLM/ATM interaction is intriguing since it adds to the list of syndromes featuring genome instability and cancer predisposition whose gene products overlap functionally. Extensive overlap exists in the phenotypes of A-T and NBS, and recent data demonstrate that Nbs1 is phosphorylated by ATM and that this modification is essential for the cellular response to DNA damage (23–25, 43, 44). Mutations in Mre11, part of the complex with Nbs1, give rise to an A-T-like syndrome featuring radiosensitivity, radioresistant DNA synthesis, and chromosome fragility (22). These data reveal that ATM and the Mre11/Rad50/Nbs1 complex operate in the same DNA damage response pathway(s) and give rise to three syndromes in the chromosomal breakage category. A new interaction, BLM with ATM, is now included in this list and adds another dimension of complexity to the recognition of abnormal structures in DNA during aberrant replication and/or in response to DNA damage.

As observed with a number of other substrates, interaction of BLM with ATM is complex, occurring with the kinase domain and the N terminus of ATM. The interaction with the N terminus region of ATM was narrowed to a minimal region of 8 amino acids (VSAS-TQAS, 82–89). This sequence also corresponds to the minimal region for p53 and BRCA1 binding (30, 40).<sup>2</sup> Since this region of ATM bound most strongly to BLM and since the helicase domain of BLM bound ATM tightly, it is possible that these regions interact, allowing ATM to bind and phosphorylate Thr-99 and Thr-122 at the N terminus of BLM. More detailed mapping of these interactions sites requires further studies. The results described here reveal that ATM interacts with and directly phosphorylates BLM on Thr-99 and Thr-122 near the N terminus of the protein. These phosphorylations are physiologically significant since expression of mutant forms fails to correct radiation-induced damage in BS cells and enhanced radiosensitivity and chromosome aberrations in control cells. What is intriguing about these mutations of BLM is that they do not predispose to elevated SCE. In essence, we have demonstrated that specific mutations near the N terminus of BLM render the cells susceptible to radiation damage at least in part by interference with the function of ATM kinase and that this is separate from the helicase activity of BLM which is required for the prevention of SCE (2). Thus it appears that BLM is involved in maintaining genome stability in different pathways, one of which is ATM-dependent. The dominant interfering effect of the BLM mutants in normal cells can be explained by mutant protein interacting with BLM partner proteins critical for maintaining DNA integrity. The BASC complex, which contains several proteins involved in maintaining genome stability, represents one such target (17). Some of the heterogene-

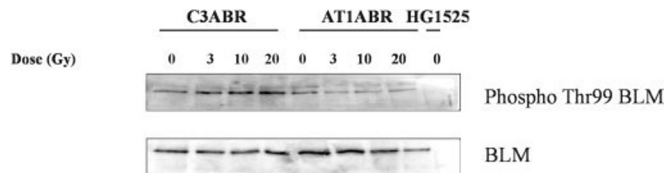


**FIG. 5. Radiation-induced phosphorylation of BLM on Thr-99 is ATM-dependent.** Upper lane, extracts from unirradiated and irradiated C3ABR and AT1ABR cells were immunoprecipitated with an antibody specific for Thr-99 phosphorylated BLM. Protein was separated on 6% SDS-PAGE and immunoblotted with anti-BLM antibody. Lower lane, immunoprecipitation of BLM from C3ABR and AT1ABR extracts with anti-BLM antibody followed by immunoblotting with the same antibody. Gy, grays.

<sup>2</sup> H. Beamish, P. Kedar, H. Kaneko, P. Chen, T. Fukao, C. Peng, S. Beresten, N. Gueven, D. Purdie, S. Lees-Miller, N. Ellis, N. Kondo, and M. F. Lavin, unpublished data.

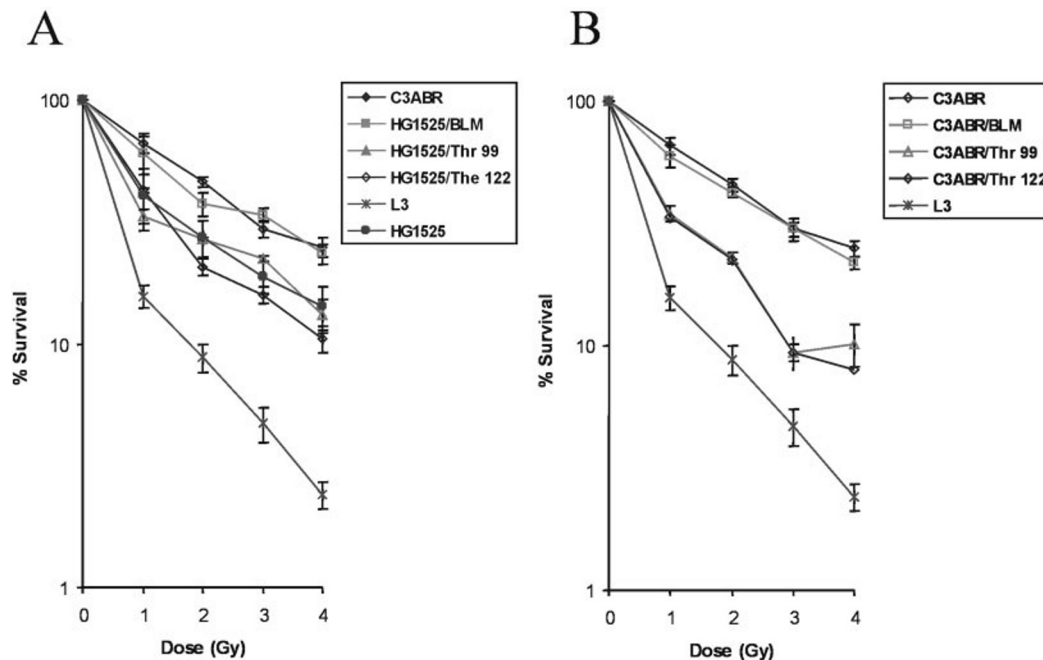


**FIG. 6. Effect of phosphorylation site mutants of BLM on radiation-induced cell survival in transfected BS and control cells.** A, cell survival in HG1525 cells transfected with BLM constructs. The BS line HG1525 was transfected with full-length BLM cDNA or the Thr-99 and Thr-122 mutants, and stable cell lines were established. Cell survival was determined at day 3 after irradiation by trypan blue exclusion. C3ABR (normal) and L3, an A-T cell line, were used as controls. Gy, grays. B, cell survival in C3ABR cells transfected with BLM constructs. The control cell line C3ABR was transfected with full-length BLM cDNA or the Thr-99 and Thr-122 mutant forms, and stable cell lines were established. Cells were irradiated and survival determined.

ity observed in BS patients might be explained by the presence of mutant protein. However, more than 90% of patients have mutations predicted to give rise to truncated protein, which is highly unstable and unlikely to cause interference with other functions. We have also demonstrated that radiation enhances the amount of Thr-99 phosphorylated BLM with increasing doses. Furthermore, this increase was defective in A-T cells, implicating ATM in this process. Thus in addition to phosphorylating BLM *in vitro*, ATM is also responsible for radiation-induced phosphorylation *in vivo*. It is not clear whether this is direct or mediated through another kinase, but based on our observations that these two proteins interact, it points to BLM being a substrate for ATM in response to DNA damage, joining an ever growing list of other substrates (45). Ababou *et al.* (46) have shown previously that BLM is retarded in its migration on SDS-PAGE in response to radiation and that phosphatase treatment restored migration to normal, providing evidence for radiation-induced phosphorylation. They also demonstrated that this shift was ATM-dependent but did not identify the site of phosphorylation. In addition to the radiation-induced phosphorylation of BLM, Ababou *et al.* (46) observed an increase in BLM protein at 8 and 24 h post-irradiation. This differs from other results in which BLM is rapidly degraded in cells undergoing DNA damage-induced apoptosis (47), and we saw some evidence of this in A-T cells (Fig. 5). It is also noteworthy that the basal level of ATM kinase activity is elevated in the BS cell line HG2703 (Fig. 4D). This is also the case for two other BS cell lines (results not shown) and may be explained by the inherent genomic instability of these cells. This explanation is supported by recent observations that 84% of undamaged BS cells contained Rad51 foci (48). Since these foci normally occur in response to radiation-induced double strand breaks in DNA, it seems likely that BS cells contain constitutively high levels of DNA breaks responsible for activation of ATM kinase. What is more difficult to explain is the reduction in ATM kinase at short times after irradiation in BS cells (Fig. 4D), which suggests that BLM may have a modulating role on ATM kinase.

Recent data reveal that BLM is required for correct relocalization of the Mre11/Rad50/nibrin complex at sites of stalled replication forks after treatment with hydroxyurea (49). Furthermore, ATR phosphorylates BLM, and this is positively correlated with the accurate subnuclear relocalization of the Mre11/Rad50/nibrin complex after hydroxyurea treatment. In the model proposed, BLM associates with stalled replication forks and assists in the loading of the Mre11/Rad50/nibrin complex. Phosphorylation of BLM by ATR facilitates recognition of the lesion, eventually leading to resolution of the stalled replication fork. Since relocalization of the complex reaches a maximum by 8 h, the timing involved raises the issue of the importance of this complex formation as a primary event in resolving the blocked fork. Hyperphosphorylation of BLM during mitosis is at least partially dependent upon ATM, and it is of interest as to whether ATR also plays a role in this process. The functional interaction between ATM and BLM during S phase in response to abnormal DNA structures and in mitosis, as well as the possible overlap in sites of phosphorylation for these different processes, requires further investigation. The presence of ATM, ATR, and BLM in complexes together with DNA damage recognition and repair proteins provides a vehicle for the functional coordination of these activities for the maintenance of genome integrity.

**Acknowledgments**—We thank Nirmala Pandeya for assistance with the statistical calculations and Tracey Laing for typing the manuscript.

## REFERENCES

- German, J. (1993) *Medicine (Baltimore)* **72**, 393–406
- Ellis, N. A., Lennon, D. J., Proytcheva, M., Alhadeff, B., Henderson, E. E., and German, J. (1995) *Am. J. Hum. Genet.* **57**, 1019–1027
- Hand, R., and German, J. (1975) *Proc. Natl. Acad. Sci. U. S. A.* **72**, 758–762
- Lonn, U., Lonn, S., Nylen, U., Winblad, G., and German, J. (1990) *Cancer Res.* **50**, 3141–3145
- Kurihara, T., Tatsumi, K., Takahashi, H., and Inoue, M. (1987) *Mutat. Res.* **183**, 197–202
- Aurias, A., Antoine, J. L., Assathiany, R., Odievre, M., and Dutrillaux, B. (1985) *Cancer Genet. Cytogenet.* **16**, 131–136
- Gangloff, S., McDonald, J. P., Bendixen, C., Arthur, L., and Rothstein, R. (1994) *Mol. Cell. Biol.* **14**, 8391–8398
- Yu, C. E., Oshima, J., Fu, Y. H., Wijsman, E. M., Hisama, F., Alisch, R., Matthews, S., Nakura, J., Miki, T., Ouais, S., Martin, G. M., Mulligan, J., and Schellenberg, G. D. (1996) *Science* **272**, 258–262
- Stewart, E., Chapman, C. R., Al-Khodairy, F., Carr, A. M., and Enoch, T. (1997) *EMBO J.* **16**, 2682–2692
- Karow, J. K., Chakraverty, R. K., and Hickson, I. D. (1997) *J. Biol. Chem.* **272**, 30611–30614
- Neff, N. F., Ellis, N. A., Ye, T. Z., Noonan, J., Huang, K., Sanz, M., and Proytcheva, M. (1999) *Mol. Biol. Cell* **10**, 665–676
- Ishov, A. M., Sotnikov, A. G., Negorev, D., Vladimirova, O. V., Neff, N., Kamitani, T., Yeh, E. T., Strauss, J. F., and Maul, G. G. (1999) *J. Cell Biol.* **147**, 221–234
- Yankiwski, V., Marciniak, R. A., Guarente, L., and Neff, N. F. (2000) *Proc. Natl. Acad. Sci. U. S. A.* **97**, 5214–5219
- Dutertre, S., Ababou, M., Onclercq, R., Delic, J., Chatton, B., Jaulin, C., and Amor-Gueret, M. (2000) *Oncogene* **19**, 2731–2738
- Liao, S., Graham, J., and Yan, H. (2000) *Genes Dev.* **14**, 2570–2575
- Wang, W., Seki, M., Narita, Y., Sonoda, E., Takeda, S., Yamada, K., Masuko, T., Katada, T., and Enomoto, T. (2000) *EMBO J.* **19**, 3428–3435
- Wang, Y., Cortez, D., Yazdi, P., Neff, N., Elledge, S. J., and Oin, J. (2000) *Genes Dev.* **14**, 927–939
- Savitsky, K., Bar-Shira, A., Gilad, S., Rotman, G., Ziv, Y., Vanagaite, L., Tagle, D. A., Smith, S., Uziel, T., Sfez, S., Ashkenazi, M., Pecker, I., Harnik, R., Patanjali, S. R., Simmons, A., Frydman, M., Sartiel, A., Gatti, R. A., Chessa, L., Sanal, O., Lavin, M. F., Jaspers, N. G. J., Malcolm, A., Taylor, R., Arlett, C. F., Miki, T., Weissman, S. M., Lovett, M., Collins, F. S., and Shiloh, Y. (1995) *Science* **268**, 1749–1753
- Carney, J. P., Maser, R. S., Olivares, H., Davis, E. M., Le Beau, M., Yates, J. R., Hays, L., Morgan, W. F., and Petrini, J. H. (1998) *Cell* **93**, 477–486
- Matsuura, S., Tauchi, H., Nakamura, A., Kondo, N., Sakamoto, S., Endo, S., Smeets, D., Solder, B., Belohradsky, B. H., Der Kaloustian, V. M., Oshimura, M., Isomura, M., Nakamura, Y., and Komatsu, K. (1998) *Nat. Genet.* **19**, 179–181
- Varon, R., Wissinger, C., Platzer, M., Cerosaletti, K. M., Chrzanowska, K. H., Saar, K., Beckmann, G., Seemanova, E., Cooper, P. R., Nowak, N. J., Stumm, M., Weemaes, C. M., Gatti, R. A., Wilson, R. K., Digweed, M., Rosenthal, A., Sperling, K., Concannon, P., and Reis, A. (1998) *Cell* **93**, 467–476
- Stewart, G. S., Maser, R. S., Stankovic, T., Bressan, D. A., Kaplan, M. I., Jaspers, N. G., Raams, A., Byrd, P. J., Petrini, J. H., and Taylor, A. M. (1999) *Cell* **99**, 577–587
- Gatei, M., Young, D., Cerosaletti, K. M., Desai-Mehta, A., Spring, K., Kozlov, S., Lavin, M. F., Gatti, R. A., Concannon, P., and Khanna, K. (2000) *Nat. Genet.* **25**, 115–119
- Dong, Z., Zhong, Q., and Chen, P. L. (1999) *J. Biol. Chem.* **274**, 19513–19516
- Zhao, S., Weng, Y. C., Yuan, S. S., Lin, Y. T., Hsu, H. C., Lin, S. C., Gerbino, E., Song, M. H., Zdzienicka, M. Z., Gatti, R. A., Shay, J. W., Ziv, Y., Shiloh, Y., and Lee, E. Y. (2000) *Nature* **405**, 473–477
- Shiloh, Y. (2001) *Biochem. Soc. Trans.* **29**, 661–666
- Abraham, R. T. (2001) *Genes Dev.* **15**, 2177–2196
- Banin, S., Moyal, L., Shieh, S.-Y., Taya, Y., Anderson, C. W., Chessa, L., Smorodinsky, N. I., Prives, C., Reiss, Y., Shiloh, Y., and Ziv, Y. (1998) *Science* **281**, 1647–1677
- Canman, C. E., Lim, D. S., Cimprich, K. A., Taya, Y., Tamai, K., Sakaguchi, K., Appella, E., Kastan, M. B., and Siliciano, J. D. (1998) *Science* **281**, 1677–1679
- Khanna, K. K., Keating, K. E., Kozlov, S., Scott, S., Gatei, M., Hobson, K., Taya, Y., Gabrielli, B., Chan, D., Lees-Miller, S. P., and Lavin, M. F. (1998) *Nat. Genet.* **20**, 398–400
- Chebab, N. H., Malikzay, A., Stavridi, E. S., and Halazonetis, T. D. (1999) *Proc. Natl. Acad. Sci. U. S. A.* **96**, 13777–13782
- Matsuoka, S., Rotman, G., Ogawa, A., Shiloh, Y., Tamai, K., and Elledge, S. J. (2000) *Proc. Natl. Acad. Sci. U. S. A.* **97**, 10389–10394
- Kastan, M. B., Zhan, Q., el-Deiry, W. S., Carrier, F., Jacks, T., Walsh, W. V., Plunkett, B. S., Vogelstein, B., and Fornace, A. J. (1992) *Cell* **71**, 587–597
- Buscemi, G., Savio, C., Zannini, L., Micciche, F., Masnada, D., Nakanishi, M., Tauchi, H., Komatsu, K., Mizutani, S., Khanna, K., Chen, P., Concannon, P., Chessa, L., and Delia, D. (2001) *Mol. Cell. Biol.* **21**, 5214–5222
- Beamish, H., and Lavin, M. F. (1994) *Int. J. Radiat. Biol.* **65**, 175–184
- Xu, B., Kim, S. T., and Kastan, M. B. (2001) *Mol. Cell. Biol.* **21**, 3445–3450
- Zhang, N., Chen, P., Khanna, K. K., Scott, S., Gatei, M., Kozlov, S., Waters, D., Spring, K., Yen, T., and Lavin, M. F. (1997) *Proc. Natl. Acad. Sci. U. S. A.* **94**, 8021–8026
- Karow, J. K., Newman, R. H., Freemont, P. S., and Hickson, I. D. (1999) *Curr. Biol.* **9**, 597–600
- Gilad, S., Khosravi, R., Shkedy, D., Uziel, T., Ziv, Y., Savitsky, K., Rotman, G., Smith, S., Chessa, L., Jorgensen, T. J., Harnik, R., Frydman, M., Sanal, O., Portnoi, S., Goldwicz, Z., Jaspers, N. G. J., Gatti, R. A., Lenoir, G., Lavin, M. F., Tatsumi, K., Wegner, R. D., Shiloh, Y., and Bar-Shira, A. (1996)



- Hum. Mol. Genet.* **5**, 433–439
40. Gatei, M., Scott, S. P., Filippovitch, I., Soronika, N., Lavin, M. F., Weber, B., and Khanna, K. K. (2000) *Cancer Res.* **60**, 3299–3304
41. Lavin, M. F., and Shiloh, Y. (1997) *Annu. Rev. Immunol.* **15**, 177–202
42. Kim, S. T., Lim, D. S., Canman, C. E., and Kastan, M. B. (1999) *J. Biol. Chem.* **274**, 37538–37543
43. Lim, D. S., Kim, S. T., Xu, B., Maser, R. S., Lin, J., Petrini, J. H., and Kastan, M. B. (2000) *Nature* **404**, 613–617
44. Wu, X., Ranganathan, V., Weisman, D. S., Heine, W. F., Ciccone, D. N., O'Neill, T. B., Crick, K. E., Pierce, K. A., Lane, W. S., Rathbun, G., and Livingston, D. M. (2000) *Nature* **405**, 477–482
45. Kastan, M. B., Lim, D. S., Kim, S. T., and Yang, D. (2001) *Acta Oncol.* **40**, 686–688
46. Ababou, M., Dutertre, S., Lecluse, Y., Onclercq, R., Chatton, B., and Amor-Gueret, M. (2000) *Oncogene* **19**, 5955–5963
47. Bischof, O., Kim, S. H., Irving, J., Beresten, S., Ellis, N. A., and Campisi, J. (2001) *J. Cell Biol.* **153**, 367–380
48. Wu, L., Davies, S. L., Levitt, N. C., and Hickson, I. D. (2001) *J. Biol. Chem.* **276**, 19375–19381
49. Franchitto, A., and Pichierri, P. (2002) *J. Cell Biol.* **157**, 19–30